faintest optical counterparts (Koekemoer et al., 2002). The whole CDFS will soon be covered by an extensive set of pointings with the new Advanced Camera for Surveys (ACS) in BVIz to "near HDF" depth. Following up the deep EIS survey in the CDFS, ESO has started a large program to image the GOODS area with the VLT to obtain deep JHKs images in some 32 ISAAC fields. The first imaging data covering the central 50 arcmin^2 have recently been made public. Optical spectroscopy across the whole field will be obtained with very high efficiency using VIRMOS on the VLT.

The multiwavelength coverage of the field will be complemented by deep radio data from the VLA at 6 cm (already obtained) and ATCA at 20 cm. The CDFS/GOODS will therefore ultimately be one of the patches in the sky providing a combination of the widest and deepest coverage at all wavelengths and thus a legacy for the future.

References

Alexander D.M., Aussel H., Bauer F.E., et al., 2002, ApJ 568, L85
Arnouts S., Vandame B., Benoist C., et al., 2001, A&A. 379, 740
Barger, A. J., Cowie, L. L., Mushotzky, R. F., Richards, E. A., 2001, AJ 121, 662
Brandt W.N., Alexander D.M., Bauer, F.E., Hornschemeier A.E., 2002, astro-ph/0202311
Cimatti, A., Daddi E., Mignoli M., et al., 2002, A&A 381, L.68
Comastri, A.; Setti, G.; Zamorani, G.; Hasinger, G., 1995, A&A 296, 1
Fabian A.C., Barcons X., Almaini O., Iwasawa K., 1998, MNRAS 297, L11
Fadda D., Flores H., Hasinger G., 2002, A&A 383, 838Fiore F., La Franca F., Giommi P., et al., 1999, MNRAS 306, 55
Franceschini A., Fadda D., Cesarsky C., et al., 2002, ApJ 568, 470
Gebhardt K., Bender R., Bower G., et al., 2000, ApJ 539, 13Giacconi, R., Rosati P., Tozzi P., et al., 2001, ApJ 551, 624
Gilli, R., Salvati, M., Hasinger, G., 2001, A&A 366, 407
Granato G.L., Danese L., Francheschini A., 1997, ApJ 486, 147
Haiman, Z. & Loeb A., 1999, ApJ 519, 479
Hasinger, G., Burg, R., Giacconi, R., et al., 1998, A&A 329, 482
Hasinger, G., Altieri, B., Arnaud, M., et al., 2001, A&A 365, 45
Hornschemeier, A.E., Brandt, W.N., Garmire, G.P., et al., 2000, ApJ 541
Hughes D.H., Serjeant S., Dunlop J., et al., 1998, Nature 394, 241
Koekemoer A.M., Grogin N.A., Schreier E.J., 2002, ApJ 567, 657
Lehmann, I., Hasinger, G., Schmidt, M., et al., 2001, A&A 371, 833
Lehmann I., Hasinger G., Murray S.S, Schmidt M., 2002, astro-ph/0109172
Mainieri V., Bergeron J., Rosati P., et al., 2002, astro-ph/0202211
Miyaji, T., Hasinger, G., Schmidt, M., 2000, A&A 353, 25
Mushotzky, R.F., Cowie L.L., Barger, A.J., Arnaud, K.A., 2000, Nature 404, 459
Norman C., Hasinger G., Giacconi R., et al. 2002, ApJ 571, 218
Rosati P., Tozzi P., Giacconi R., et al., 2002, ApJ 566, 667
Schmidt, M., Schneider, D.P. \& Gunn J.E., 1995, AJ 114, 36
Schmidt, M., Hasinger, G., Gunn, J.E., et al., 1998, A&A 329, 495
Schneider, D.P., Schmidt, M., Hasinger, G., et al., 1998, AJ 115, 1230
Shaver P.A. et al., 1996, Nature 384, 439
Steidel C.C., Adelberger K.L., Giavalisco M., Dickinson M., Pettini M., 1999, ApJ 519, 1
Stern D., Moran E.C., Coil A.L., et al., 2002, ApJ 568, 71
Szokoly, G., Hasinger G., Rosati, P. et al., 2002 (in prep.)
Vandame et al. 2001, astro-ph/0102300
Vignati P., Molendi S., Matt G., et al., 1999, A&A 349, L57

Using color-magnitude diagrams and spectroscopy to derive star formation histories: VLT observations of Fornax

CARME GALLART[1], Andes Prize Fellow, Departamento de Astronomía, Universidad de Chile, and Department of Astronomy, Yale University
ROBERT ZINN, Department of Astronomy, Yale University
FREDERIC PONT[2], Departamento de Astronomía, Universidad de Chile
EDUARDO HARDY, National Radio Astronomy Observatory
GIANNI MARCONI, European Southern Observatory
ROBERTO BUONANNO, Osservatorio Astronomico di Roma

1. Star formation and chemical enrichment histories of the Milky Way satellites

During the last decade, the varied star formation histories of the dSph galaxies satellites of the Milky Way have been revealed to us in detail, dramatically changing our perception from the early idea that they were predominantly old systems. Some hints on the presence of, at least, an intermediate-age population had been provided previously by the peculiarity of the variable star populations of dSph galaxies (Norris & Zinn 1975) and the discovery of Carbon stars in Fornax (Demers & Kunkel 1979; Aaronson & Mould 1980), Carina (Cannon, Niss & Norgaard-Nielsen 1981) and other dSph (Aaronson, Olszewski & Hodge 1983). However, only in the last few years have these intermediate-age populations been shown beautifully in the wide-field, extremely deep CMDs of a number of dSph galaxies. There is the extreme case of Leo I (Caputo et al. 1999; Gallart et al. 1999a,b), which has formed over 80% of its stars from 6 to 1 Gyr ago, and the intermediate cases of Carina (Smecker-Hane et al. 1996; Hurley-Keller et al. 1998; Castellani et al. 2001) and Fornax (Stetson et al. 1997; Buonanno et al. 1999), with prominent intermediate-age populations. There are also predominantly old systems like Draco (Aparicio et al. 2001) and Ursa Minor (Carrera et al. 2002).

These CMDs offer qualitative first glances at the star formation histories (e.g. in the case of Carina, one can see that there have been three major events of star formation), but their quantitative determination requires a detailed comparison of the distribution of stars in the CMD with that predicted by model CMDs. CMDs reaching the old main-sequence turnoffs are particularly useful for these comparisons because there are few uncertainties in the theory for this stage of a star's life and there is less age-metallicity degeneracy. We have shown that with this method, it is possible to break the classical age-metallicity degeneracy in stellar populations for systems with low levels of metal enrichment like Leo I (Gallart et al. 1999b). However, in the case of a more complicated chemical

[1]Currently: Ramon y Cajal Fellow. Instituto de Astrofísica de Canarias.
[2]Currently: Observatoire de Genève.

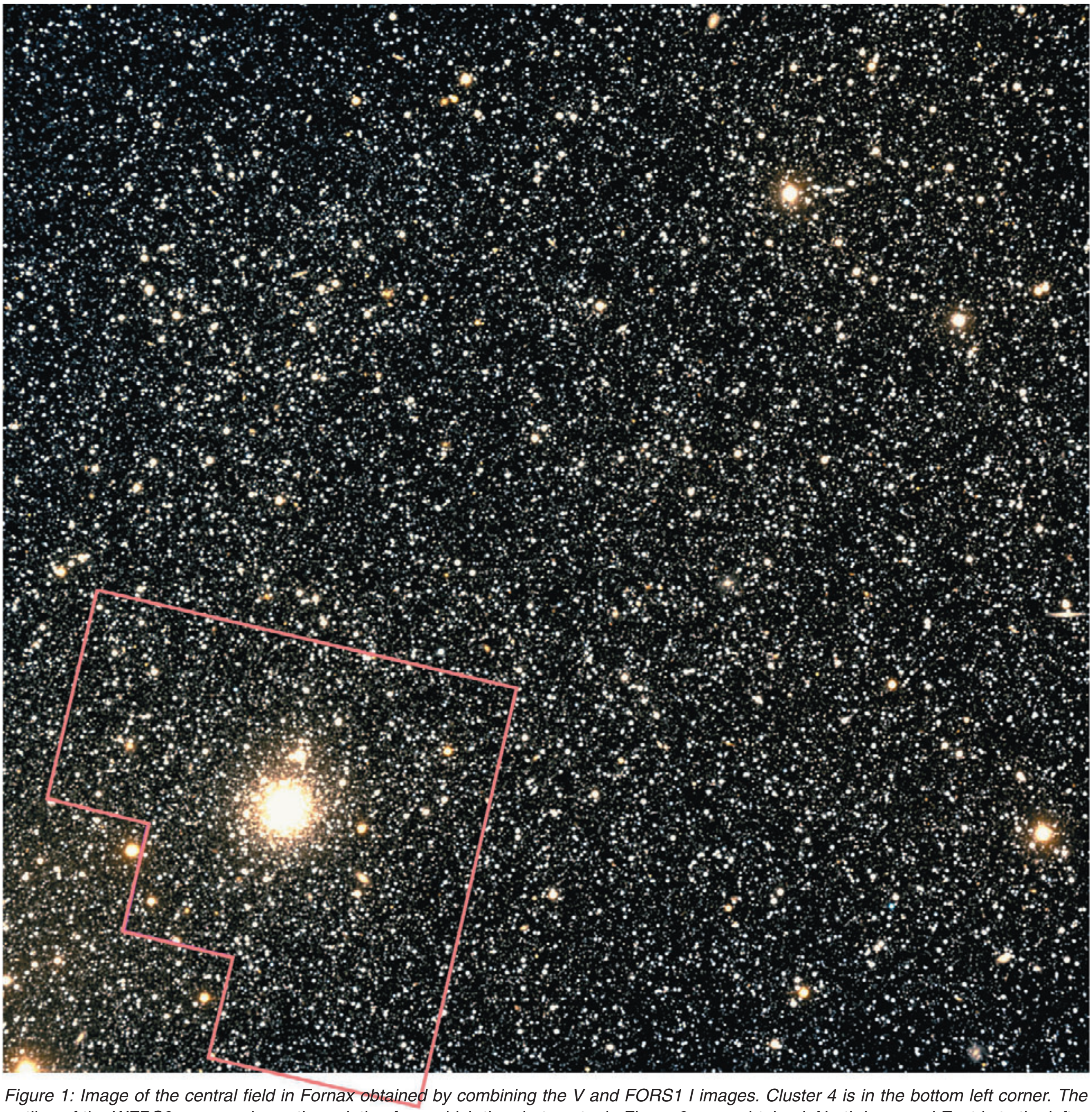

Figure 1: Image of the central field in Fornax obtained by combining the V and FORS1 I images. Cluster 4 is in the bottom left corner. The outline of the WFPC2 camera shows the pointing from which the photometry in Figure 2c was obtained. North is up and East is to the left.

evolution, the age-metallicity degeneracy may be more difficult to break (Gallart, Aparicio & Bertelli 2002), and in these cases, obtaining independent constraints on the age-metallicity relationship $Z(t)$ may be key to retrieving unambiguously the star formation history.

Spectroscopic studies that would provide direct information on the metallicities of the stars in these galaxies are scarce, due to the large investment of large-aperture telescope time required. Only a few high dispersion spectroscopic studies of stars in dSph galaxies have been published so far, either from Keck-HIRES (e.g. Shetrone, Côté & Sargent 2001 and references therein) or from VLT-UVES (Bonifacio et al. 2000), and all count the measured stars by the units. The extraordinary multiplexing capability of FLAMES at the VLT will certainly cause a breakthrough in this field in the near future.

A more economical – though less informative – way of obtaining metallicity information involves low resolution spectroscopy. The Ca II triplet offers the possibility of obtaining global [Fe/H] values for individual stars with relatively high precision (≤ 0.2 dex), and this technique has developed into the most popular way of using low-resolution spectra to estimate the abundances of stars in globular clusters and dSph galaxies.

We undertook a study of the star formation and chemical enrichment history of the Fornax dSph galaxy with the twofold approach described above: we used the VLT with FORS1 to obtain photometry reaching the oldest main-sequence turnoffs and CaII triplet spectroscopy of a sample of red giant branch stars in the same fields. The observations and the main results are described below.

2. Wide field color-magnitude diagrams

We obtained old main-sequence turnoff photometry in three fields at two galactocentric distances in the dSph Fornax, using FORS1 at the VLT. The observations were performed in service mode in July 2000, with the requirement of seeing ≤ 0.6″, which is key to perform photometry in fields affected by stellar crowding. In some of the frames,

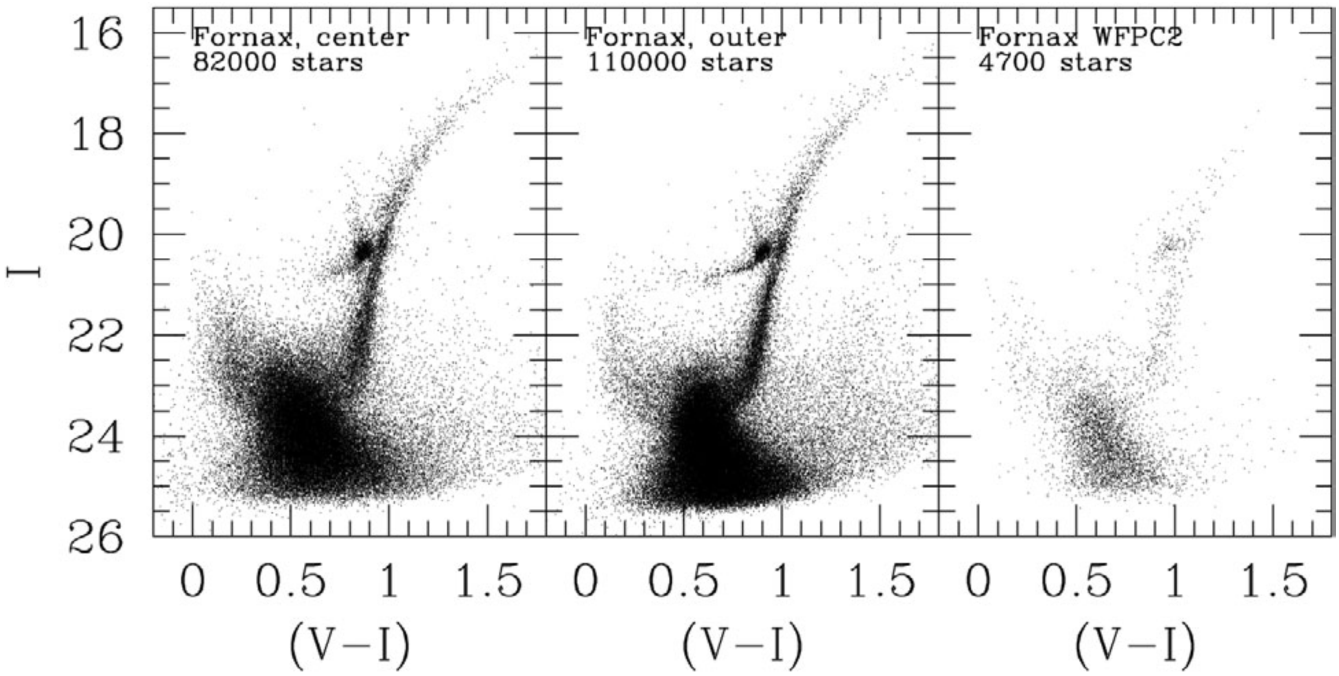

Figure 2: a) CMD for a FORS1 field centred in Fornax; b) composite CMD for the two fields situated about 11 arcmin North; c) WFPC2 CMD of a subset of the central field, shown in Figure 1.

with exposure times as long as 750 sec, the seeing was measured as good as 0.4″. In the central field, containing globular cluster Fornax #4, a total of 3650 sec in V and 4700 sec in I were accumulated. The other two fields were situated at about 11 arcmin north of the center of the galaxy, and total integration times were 1850 sec in V and 4600 sec in I. The locations of these off-center fields were chosen by considering the change in surface brightness across Fornax and then selecting fields that would provide measurements of similar numbers of stars in the central field and in the other two fields combined. A composite image combining the V and I frames of the central field is shown in Figure 1, where the outline of the HST WFPC2 camera has been superimposed in the position where HST observations exist. The gain in area allowed by FORS1 at the VLT is key to measuring sufficient numbers of stars in parts of the CMD that are vital for deriving the star formation history, such as the subgiant branch and the horizontal branch.

Figure 2 shows the CMDs at the two galactocentric distances. The CMD in Figure 2a corresponds to the central field, while Figure 2b displays the CMD of the off-center fields. Figure 2c shows the WFPC2 CMD from Buonanno et al. (1999). Note that the depth of the FORS1 CMDs is similar to that of the WFPC2 CMD, but that the number of stars in the former is much larger, thus providing a better representation of the star formation history, not affected by small number statistics. In fact, a tantalizing evidence of bursts of star formation in Fornax was provided by the sparsely populated subgiant branch of the WFPC2 CMD; the FORS1 CMD, instead, seems to shows a smooth distribution of stars in the subgiant branch, that may be indicative of continuous star formation. We are still investigating if we can definitely rule out discrete burst of star formation with the FORS1 data.

Our goal is to derive the complete star formation history in these fields, and test for possible spatial variations, using synthetic CMDs, and the input on $Z(t)$ from the Ca II triplet study (see below).

3. Stellar metallicities from the Ca II triplet

We obtained Ca II triplet spectroscopy for about 100 RGB stars in the central part of Fornax, using FORS1 at the VLT, in December 1999. The central wavelength was 7490 Å, dispersion 1.06 Å per pixel, and resolution $R \simeq 1530$. The excellent seeing conditions during the observations – most of the time below 0.8″ seeing – allowed us to use slitlet widths of 0.7 arcsec. We observed seven fields, with an average of 17 targets per field. For each, two 20-min exposures were acquired on two positions offset along the slit by about 3″. This procedure allows the direct substraction of the sky from the unextracted spectra and very significantly improves the removal of the contamination by night sky emission lines. Short expo-

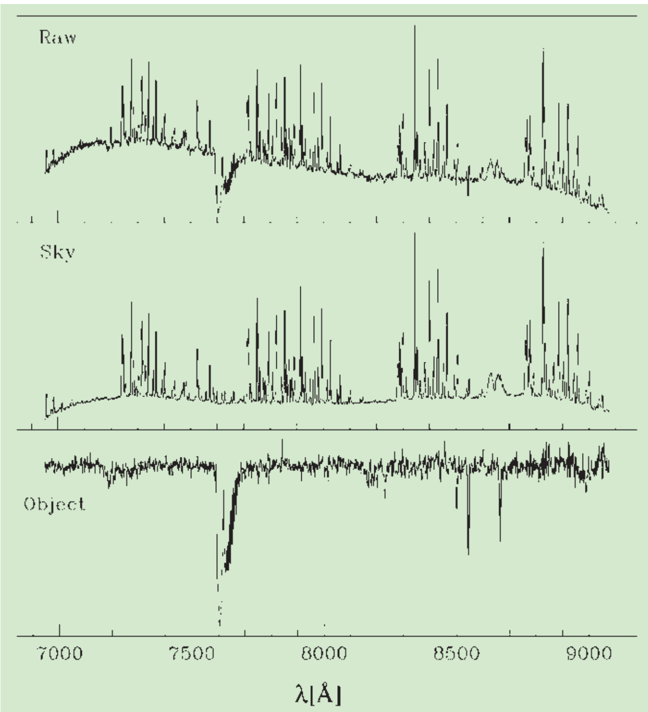

Figure 3: Example showing the excellent sky subtraction allowed by the dithering technique in one of our Fornax targets. Top: raw spectrum. The sky emission lines are prominent, with the Ca II triplet lines hardly noticeable under them. Middle: the sky spectrum obtained next to the star spectrum. Bottom: the final sky-subtracted spectrum.

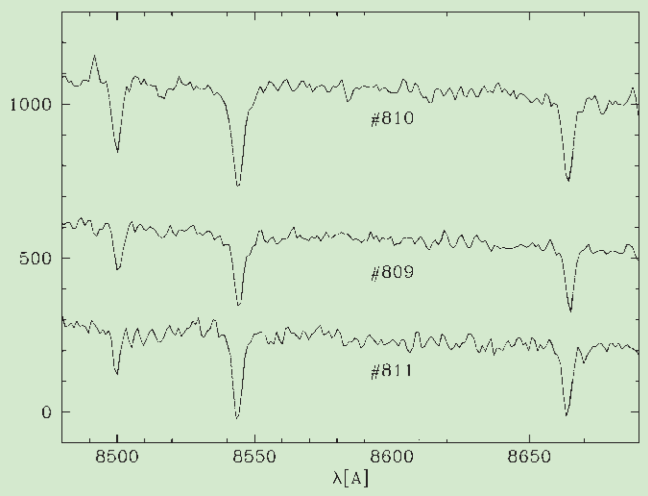

Figure 4: Representative spectra for three stars spanning the luminosity range of our targets.

sures were also obtained on selected red giants of three nearby globular clusters of known metallicity for calibration purposes.

Figure 3 show the excellent sky substraction that can be achieved with the dithering technique discussed above. Figure 4 shows three examples of the quality of the spectra obtained for one of the brightest, faintest and intermediate-brightness stars in our sample.

We find a large metallicity dispersion in Fornax, with about 20% of the objects having low abundances (–2.5 ≤ [Fe/H] ≤ –1.3), and about 35% having abundances greater than 47 Tuc ([Fe/H] = –0.7). The peak of the metallicity distribution occurs at [Fe/H] ≃ –0.9. The most metal rich stars have Ca II triplet equivalent widths W(Ca) as strong as the average of the metal-richer LMC population in Cole et al. (2000). This allows us to put an upper limit to the metallicity of the stars in Fornax, which lie in a somewhat uncertain area of the *W*(Ca)-[Fe/H] calibration (see Pont et al. 2002 for a thorough discussion of this point).

The combination of the spectroscopic metallicity for each star with its color on the RGB provides a constraint on its age, and therefore, a well delineated age-metallicity relation can be obtained, especially for the more metal-rich, young stars. The colors of most metal-rich RGB stars are much bluer than those of an old globular cluster of the same metallicity, and lead to the conclusion that they must be much younger. Indeed, while for each given metallicity, stars older than ≃ 3 Gyr have a small range in color, the younger stars are substantially and increasingly bluer with decreasing age. In Figure 5 we display a preliminary version of the Fornax age-metallicity relation obtained by Pont et al. (2002).

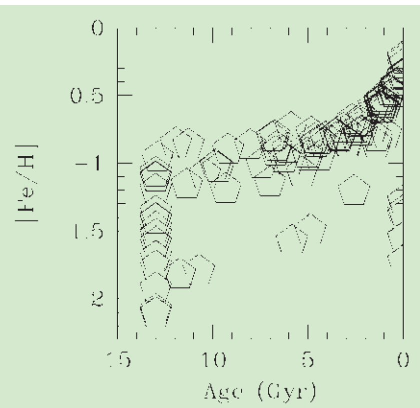

Figure 5: Age-metallicity relation obtained for Fornax from Ca II triplet spectroscopy and RGB photometry. See text for details.

Finally, using theoretical evolutionary models, we investigated the relation between the stellar population represented in the fraction of the RGB that has been spectroscopically observed, and the total population of the galaxy.

4. Combining Ca II triplet spectroscopy with the color-magnitude diagram: a coherent picture of the Fornax star formation history

The *Z*(*t*) shown in Figure 5 was obtained by combining the spectroscopic metallicity with the position of the stars on the RGB. But is our picture compatible with parts of the CMD other than the RGB? The Fornax CMD contains numerous features associated with a particular age and metallicity, namely a horizontal branch, an important red clump with a long tail at the bright end, and a main sequence extending to M_I ~ –0.5. These features indicate respectively the existence of an old, metal-poor population, a significant intermediate-age population, and a very recent population, as young as ≃500 Myr old. All of these are qualitatively compatible with the picture obtained from the RGB and the Ca II triplet, which indicates the need for a substantial amount of young population to account for the blue color of the metal-rich stars.

The locations of these evolutionary phases in the CMD depend on the metallicities and the ages of the stars (thus on *Z*(*t*)), while the numbers of stars in each phase depend on the lifetime of the phase and the star formation history of Fornax. To test if the derived *Z*(*t*) produces stars in the right positions in the CMD, we computed a synthetic model of the Fornax CMD assuming that *Z*(*t*) and a constant star formation rate starting 12 Gyr ago and stopping 600 Myr ago, to account for the absence of a very bright main sequence in the CMD. *Z*(*t*) was approximated by a linear interpolation between (Gyr ~ *z*) = (15.0,0.0001), (10,0.0011), (2, 0.0036), (1, 0.0057) and (0, 0.008). We used the synthetic CMD code ZVAR (Bertelli et al. 2002) with the Bertelli et al (1994) generation of Padova stellar evolutionary models. A Kroupa, Tout & Gilmore (1993) IMF has been assumed, and a binary fraction β = 0.25, with mass fraction *q* > 0.7 and flat IMF for the secondary stars. For a description of these parameters and the way they are used in the ZVAR code, the reader is referred

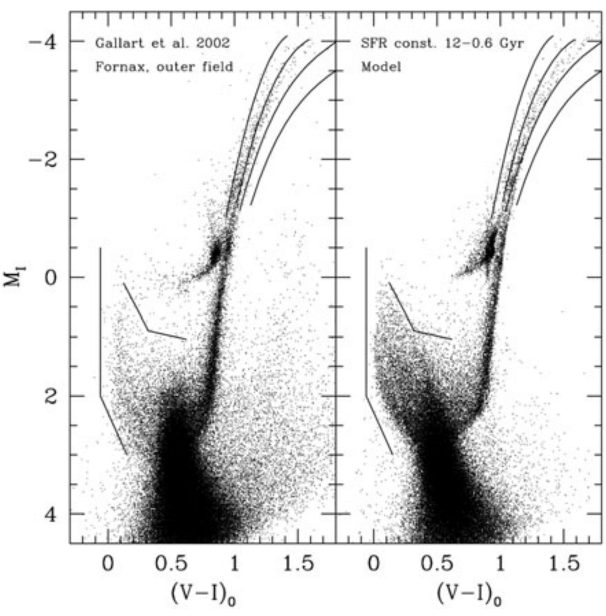

Figure 6: Observed CMD for the outer Fornax field (left) and model color-magnitude diagram (right) obtained assuming a fit to the Z(t) displayed in Figure 5, a constant star formation rate from 12 to 0.6 Gyr ago, and a given binary fraction (see text for details). A few lines around the upper main sequence, and a few globular cluster RGB loci from Da Costa & Armandroff (1990) have been drawn to guide the eye. Note that the different density of stars in different areas of the CMD may be due to the fact that the star formation rate has been assumed constant (we did not try to model it a this stage). Also the simulation of observational errors is somewhat preliminary and an underestimate of the errors may cause the different width of the main-sequence and the different shape of the red-clump.

to Gallart et al. (1999b). The completeness and error simulation has been performed using a preliminary crowding test table obtained from the deep VLT imaging for Fornax presented in Gallart et al. (2002).

The resulting synthetic CMD is displayed in Figure 6, to the right of the observed CMD. The synthetic CMD successfully reproduces the major morphological features of the observed CMD, namely the RGB, the horizontal branch, the red-clump and the main-sequence. Particularly important is the agreement between locations of the young main-sequence stars (a set of lines have been drawn in both the observed and model CMDs to guide the eye). Its position is very sensitive to metallicity of the stars younger than about 2 Gyr. If their metallicity were lower than that given by the $Z(t)$ relation, for example, lower than [Fe/H] ≤ –0.7, as one could deduce from the color of the RGB without correction for the young ages of the stars, then the position of this part of the main sequence would be substantially too blue. There is also striking agreement between the model and observed CMDs for the *plume* of stars above the red-clump, which is composed of metal rich young stars (younger than 1 Gyr and with $Z \simeq$ 0.006–0.008) undergoing their He-burning loop phase of stellar evolution. The most obvious disagreement between the model and the observed CMDs is in the color of the RGB. To illustrate this we have plotted in both diagrams the fiducial RGBs of the globular clusters M15, M2, NGC 1851 and 47 Tuc, from Da Costa & Armandroff (1990). Notice that the model RGB is somewhat redder than the observed one. This disagreement, which is larger for the fainter RGB stars, is known to exist from other comparisons between observations and the Padova stellar evolutionary models. It has no effect on our major conclusion that the $Z(t)$ shown in Figure 5 is compatible with the morphology of the Fornax CMD. A quantitative derivation of the star formation history from a thorough fit of the CMD will add further confidence in the reconstruction of the history of Fornax. It will be presented in Gallart et al. (2002).

Acknowledgements. This research is part of a Joint Project between Universidad de Chile and Yale University, funded partially by the Fundación Andes. C.G. acknowledges partial support from Chilean CONICYT through FONDECYT grant number 1990638. R.Z. was supported by NSF grant AST-9803071 and F.P. by the Swiss National Science Fund and FONDECYT grant number 3000056.

References

Aaronson, M., Olszewski, E.W. & Hodge, P.W. 1983, ApJ, **267**, 271
Aaronson, M. & Mould, J. 1980, ApJ, **240**, 804
Aparicio, A., Carrera, R. & Martínez-Delgado, D. 2001, AJ, **122**, 2524
Bertelli, G., Bressan, A., Chiosi, C., Fagotto, F. & Nasi, E. 1994, A&AS, **106**, 275
Bertelli, G. et al. 2002, in preparation
Bonifacio, P., Hill, V., Molaro, P., Pasquini, L., Di Marcantonio, P., & Santin, P. 2000, A&A, **359**, 663
Buonanno, R., Corsi, C.E., Castellani, M., Marconi, G., Fusi Pecci, F. & Zinn, R. 1999, AJ, **118**, 1671
Cannon, R.D., Niss, B. & Norgaard-Nielsen, H.U. 1981, MNRAS, **196**, 1
Caputo, F., Cassisi, S., Castellani, M., Marconi, G., Santolamazza, P. 1999, AJ, **117**, 2199
Carrera, R., Aparicio, A., Martínez-Delgado, D., & Alonso, J. 2002, AJ, in press
Castellani, M., Pulone, L., Ripepi, V., Dall'Ora, M., Bono, G., Brocato, E., Caputo, F., Castellani, V., Corsi, C. 2001,
in "Dwarf Galaxies and their environment", eds. K.S. de Boer, R.-J. Dettmar & U. Klein, Shaker Verlag.
Cole, A., Smecker-Hane, T.A., Gallagher, J.S. 2000, AJ, **120**, 1808
Da Costa, G. S. & Armandroff, T. E. 1990, AJ, **100**, 162
Demers, S. & Kunkel, W.E. 1979, PASP, **91**, 761
Gallart, C., Aparicio, A., Bertelli, G. 2002, in "Observed HR diagrams and stellar evolution...", eds. T. Lejeune & J. Fernandes, ASP Conference Series.
Gallart, C. et al. 1999a, ApJ, **514**, 665
Gallart, C., Freedman, W.L., Aparicio, A., Bertelli, G. & Chiosi, C. 1999b, AJ, **118**, 2245
Gallart, C., Zinn, R., Marconi, G., Hardy, E. & Buonanno, R. 2002, in prep.
Hurley-Keller, D., Mateo, M. & Nemec, J. 1998, AJ, **115**, 1840
Kroupa, P., Tout, C.A. & Gilmore, G. 1993, MNRAS, **262**, 545
Norris, J. & Zinn, R. 1975, ApJ, **202**, 335
Pont, F., Zinn, R., Gallart, C., Winnick, R., Hardy, E. 2002, in preparation
Shetrone, M.D., Côté, P. & Sargent, W.L.W. 2001, ApJ, **548**, 592
Smecker-Hane, T. A., Stetson, P. B., Hesser, J. E. & van den Bergh, D. A. 1996 *in From stars to galaxies*..., eds.
C. Leitherer, U. Fritze-van Alvensleben & J. Huchra. ASP Conf Ser, **98**, 328
Stetson P. B., Hesser, J. E. & Smecker-Hane, T. A. 1998,
PASP, **110**, 533

The ups and downs of a stellar surface: Nonradial pulsation modelling of rapid rotators

THOMAS RIVINIUS, DIETRICH BAADE, ESO, Garching b. München, Germany
STANISLAV ŠTEFL, Astronomical Institute, Academy of Sciences Ondřejov, Czech Republic,
MONIKA MAINTZ, Landessternwarte Heidelberg, Germany
RICHARD TOWNSEND, University College London, United Kingdom

1. Introduction

Usually one thinks of stars as stable objects, taking at least millions of years to evolve significantly. While it is true that stars take such timescales to age, they need not be "stable" in a static sense over all that time. Many stars in fact undergo pulsations on timescales between minutes and years, as for instance the Be stars Baade, Rivinius and Štefl reported about in a recent Messenger issue (No. 107, p. 24). The most obvious pulsation mode is the radial one, where the star becomes bigger and smaller periodically, and like any expanding/compressing gas also cooler and hotter again. We see these stars varying in brightness and colour, and their spectra cyclically approaching and receding. The well known Mira in the constellation Cetus P = 330 day), or the Cepheids (P = 1…50 day), which help in measuring extragalactic distances, are such objects. Stars may not only pulsate radially, however. Imagine a free-floating blob of water in a Space Shuttle, or a big soap bubble. Before reaching a stable spherical shape (or popping) they undergo damped wobbles. This, in a sense, is externally excited non-radial pulsation (*nrp*) in a multitude of modes.

Nonradially pulsating stars behave similarly. But since these pulsations are excited from inside the star and are going on for millions of cycles, they appear more ordered as most modes are damped, and typically only one or few high-amplitude modes are excited in an *nrp* star. The excitation process resembles a Carnot process (as in an ideal steam engine) where the role of the valve is played by a layer inside the star that turns opaque with increasing temperature due to ionization processes and becomes transparent again during